Journal of Power Sources 262 (2014) 192–200

Contents lists available at ScienceDirect

Journal of Power Sources

journal homepage: www.elsevier.com/locate/jpowsour

Influence of temperature on the electrokinetic properties and power generation efficiency of Nafion® 117 membranes

Jacopo Catalano, Anders Bentien*

Department of Engineering, Aarhus University, Hangøvej 2, 8200 Aarhus, Denmark

HIGHLIGHTS

- Electrokinetic energy conversion is investigated experimentally.
- High electrokinetic energy conversion efficiency in Nafion membrane is found.
- Power density and efficiency increases with temperature.
- Temperature dependence of pore size in Nafion are estimated from transport properties.

ARTICLE INFO

Article history:
Received 30 December 2013
Received in revised form
10 February 2014
Accepted 13 March 2014
Available online 22 March 2014

Keywords:
Nafion membranes
Electrokinetic energy conversion
Hydraulic permeability
Streaming potential
Ion conductivity
Pore diameter

ABSTRACT

In the present study we investigate the transport properties of Nafion® 117 membranes in temperatures ranging from ambient temperature up to 70 °C. The hydraulic permeability, streaming potential and ion conductivity have been measured as function of temperature in 0.03 M LiCl solutions in purposely designed, non-conductive set-ups. In particular, the apparent activation energies of the processes have been retrieved: 29.4 kJ mol^{-1}, 9.3 kJ mol^{-1} and 22.9 kJ mol^{-1} for the hydraulic permeability, streaming potential coefficient and ion conductivity respectively. Based on the knowledge of the temperature dependence of these three independent properties the *figure-of-merit* of the electrokinetic energy conversion process has been calculated obtaining a monotonous increase of the efficiency with temperature. At 70 °C the electrokinetic efficiency is rather high about 26.6%:50% higher with respect to the one found at room temperature. The electrokinetic transport properties were also used to esteem the average pore size of the water channels in the polymer matrix resulting in pore diameters ranging approximately from 2.0 (25 °C) to 2.8 nm (70 °C).

1. Introduction

The increasing demand of energy and the need of decentralized power generation systems combined together with the urgency of emission reductions encouraged the researchers' interests in developing new, efficient and more environmental friendly energy production systems. Polymer electrolyte fuel cells, PEMFCs, are potentially among the most efficient devices for power generation, and a large amount of specific literature has been published in the last decades focusing, especially, in developing new solid polymer electrolyte materials with enhanced properties [1–6]. However, despite the efforts devoted in this direction the reference membrane for fuel cell applications still remains Nafion®, produced by DuPont, due essentially to the high chemical, mechanical and thermal stability and high proton conductivity during fuel cells operation. Another attractive, still not well investigated, way of energy conversion in ion conductive membranes is the direct conversion of kinetic energy into electrochemical energy. The electrokinetic energy conversion has been studied both theoretically [7–10] and experimentally focusing the attention mostly on the properties of straight nanochannels with reported efficiencies up to 10% [11–16]. In literature, a few studies of the electrokinetic properties of ion conductive membranes have been reported. A non-mechanical pressurization system based on Nafion® 117, in the following referred to as Nafion, in tetrapropylammonium iodide and iodine in DMF solutions has been proposed by Evans et al. [17], while we have reported the electrokinetic properties of Nafion at room temperature in a previous work [18]. However a more systematic experimental investigation of the electrokinetic properties of ion conductive membranes is still missing. The basic mechanism behind the electrokinetic power generation is the potential

* Corresponding author.
E-mail address: bentien@eng.au.dk (A. Bentien).

http://dx.doi.org/10.1016/j.jpowsour.2014.03.042
0378-7753/

difference generated by a pressure gradient applied across a membrane, i.e. streaming potential, separating two compartments filled with aqueous solutions having the same salt concentration. The streaming potential is a consequence of the coupling between ions and solvent (hydration) and whenever a pressure difference drives a volume flux through the membrane, ions are dragged along, whereby creating a potential difference. One of the key advantages of electrokinetic energy conversion is that moving mechanical stages are not required. Nonetheless, high conversion efficiency along with high power density are fundamental parameters in comparisons to e.g. electromagnetic actuators that represent the state-of-the-art of commercially available units that convert kinetic energy into electrical energy.

Based on measurements of the hydraulic permeability (κ_H), streaming potential coefficient (ν) and ion conductivity (σ) the electrokinetic *figure-of-merit* $\beta_{EK} = \nu^2 \cdot \sigma / \kappa_H$ is retrieved and can be used for calculation of the electrokinetic conversion efficiency $\eta_{EK} = [(1+\beta_{EK})^{1/2} - 1]/[(1+\beta_{EK})^{1/2} + 1]$. For a more detailed discussion the reader is referred to refs. [7,8,16,19].

In previous studies we demonstrated that the maximum efficiency of 18 ± 2% for Nafion [18] is significantly higher with respect to the non- or low-charged membranes [16,18], for which a maximum of about 7% for Cyclopore and Nucleopore membranes has been found [16]. These results indicate that ion conductive membranes could represent a possible pathway for high-efficiency electrokinetic energy conversion. The high electrokinetic efficiency observed in ion conductive membranes with respect to non-charged membranes could be explained by the high surface charge density, $\sigma_q \sim 0.2–1$ C m^{-2} for Nafion [20,21], of the nanoporous hydrophilic network. In its swollen state, an ion exchange membrane can be depicted as a hydrophobic PTFE-like matrix and a network of more or less interconnected water nano-channels in which the transport of water and ions takes place [22–27]. Besides the fixed charge density, the electrokinetic properties of such a system strongly depend on the average pore dimensions and channel tortuosity [28,29]. Several ways to modify the pore structure of Nafion, to increase the ion exchange capacity, the water retention and the mechanical and thermal stability have been proposed in the literature. This includes e.g. addition of hygroscopic materials (Al_2O_3, SiO_2, clays, silicophosphate gels etc.) obtaining inorganic-polymer composite membranes [30], use of dendrimers [31]. On the other hand it is well known from the literature that by increasing the temperature, Nafion membranes show higher dimensional swelling [32], liquid water uptake [33–35] and hydraulic permeability [36,37]. These latter experimental evidences indicate a more open structure with higher water content and larger average pore size. It is anticipated that all the three transport properties that enter the expression for $\beta_{EK} = \nu^2 \cdot \sigma / \kappa_H$ increase with the pore dimensions and thus with temperature. Still, the expected temperature dependence of β_{EK} is not known and depends on whether the nominator ($\nu^2 \cdot \sigma$) has a larger increase with temperature with respect to the denominator (κ_H). Therefore the main objective of this work is to experimentally determine the temperature dependence of κ_H, ν and σ in Nafion membranes and to get more detailed insight on the electrokinetic conversion efficiency as function of temperature.

2. Materials and methods

2.1. Membranes

Nafion 117, with a nominal thickness of 178 μm, was bought from Ion Power Inc, US. Before use membrane samples were pretreated by boiling in demineralized water. The membranes were then heated in 3wt% of H_2O_2 water solution for 60 min at $T \sim 90$ °C, transferred in boiling demineralized water, and then heated up to 90 °C for 60 min in 0.5 M H_2SO_4 water solution. Finally the membranes were washed in warm (~70 °C) demineralized water for ten minutes; the last step was repeated four times. After pretreatment the membrane samples were stored in 0.5 M LiCl solutions to obtain Nafion in Li^+ form. All measurements have been carried out in 0.03 M LiCl aqueous solutions, and to avoid any increase in the concentration in the measurement cells the membranes were carefully rinsed in 0.03 M LiCl before being tested. The membrane thickness in both the dry and swollen states was measured with a digital micrometer (Diesella, resolution 1 μm).

2.2. Hydraulic permeability and streaming potential apparatus

The experimental set-up for the measurement of the hydraulic permeability and streaming potential as a function of the temperature is schematically shown in Fig. 1. It consists of two jacked borosilicate glass chambers of about 400 cm^3 volume separated by two membrane holders made in Teflon. The custom-made holders had 4 ports each for instruments' connection (e.g. thermocouples and electrodes). The temperatures in the two cells were independently controlled by two different water baths (Eco Gold Lauda DE, temperature stability 0.01 °C) feeding the chambers' jackets, and monitored through two thermocouples type K (Omega US, 1/16 inch) placed at approximately 5 mm from the membrane surfaces. To reduce concentration polarization at the membrane/solution interface and to have a more uniform and constant temperature, two inert magnetically coupled stirrers (Büchi CH, Cyclone *i*) have been employed. The stirrers, having all the wet parts in PFA and glass, are rated to work up to 6 bar of pressure and temperature up to 180 °C and they were connected through GL 32 ports to the two Teflon lids of the two chambers. The absence of the shaft rotation ensures a small leakage of the system which was further reduced by using an additional O-ring (Seals DK, Silicon) along the shaft axis. The two chambers were filled with identical aqueous solutions by first applying vacuum (Vacuumbrand DK rotary pump) in both chambers (valves V3, V6 and V7 close, all the others open), and, subsequently by opening the outlet valves (V1–V5 close, V6 and V7 open), which were beforehand connected with a solution reservoir. After the system reached the thermal stability the low pressure chamber was connected to a calibrated capillary and pressure was applied in the high pressure chamber by using an Ar gas cylinder (V3 and V5 open, V7 close), and was monitored, in each cell, by the use of pressure transducers (Druck DE, range 1–11 bar). The glass reactors were designed to work above 6 bar in pressure, and in order to avoid any unexpected increase two additional rupture discs (Büchi CH, wet part in graphite and PFA 6 bar) were connected to the two cells.

The active area for the membrane transport was 3.14 cm^2. To avoid any deformation of the membrane due to the applied pressure, a screen (Sartorius US, coarse grid Teflon coated stainless steel) has been used in the low pressure compartment. The streaming potential was measured through the use of two Ag/Ag–Cl electrodes (0.25 mm in diameter) placed close to the membranes surfaces and mounted through the two membranes holders with PEEK 1/16 inch connector (Mikrolab DK) and purposely designed Teflon ferrules. The electrodes were prepared from 0.25 mm diameter silver rod (Alfa Aesar DE, 99.9985% metal basis) following the same procedure reported in a previous publication [18]. The hydraulic permeability was monitored following the movement of the liquid meniscus over time in the calibrated capillary (Teflon, inner diameter 0.75 mm).

All the fitting, valves and tubing were in Teflon and bought from Swagelok, with the exception of the GL connection of the cells (PFA) and the vacuum fittings and valves which were purchased form

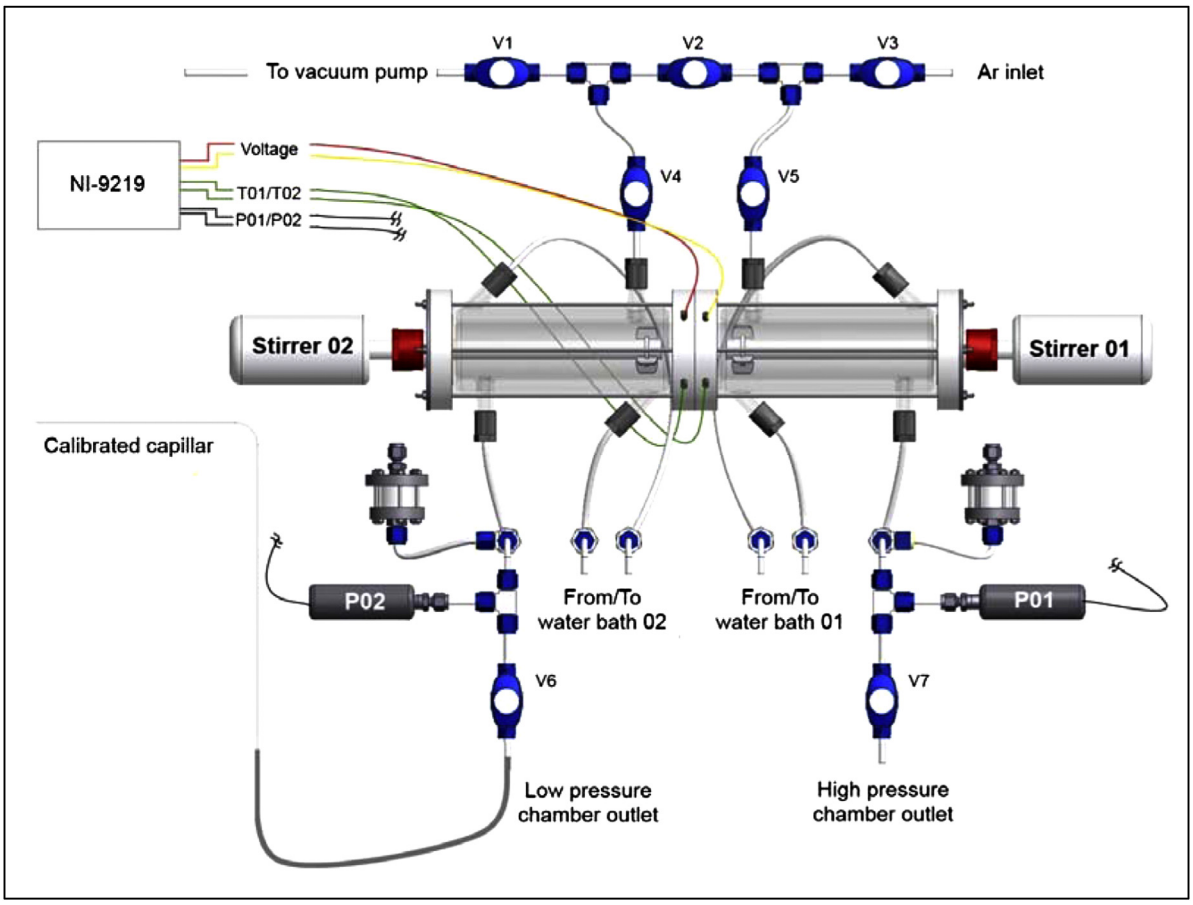

Fig. 1. Schematic of the experimental set-up used in this work for hydraulic permeability and streaming potential tests.

Bola, DE and Edwards, UK respectively. All the signals were acquired via NI-9219 acquisition card (National Instruments) at 1 Hz and monitored and recorded with Labview.

2.3. Ion conductivity through-plane and in-plane apparatuses

Ion conductivity was measured in two different set-ups. In particular through-plane measurements were carried out in the same electrochemical cell used in a previous publication [18] placed in an incubator (Binder DE, maximum temperature 100 °C); the temperature of the system was monitored with two thermocouples type K (Omega Us, 1/32 inch). Unlike the previous study, the electrodes were mounted in spring-loaded holders (sketched schematically in Fig. 2) to reduce the distance between electrodes and membrane surfaces. In this case to guarantee a more planar surface the silver rod was mounted in a tubing sleeve (Idex US, 0.4 and 0.75 mm I.D. and O.D. respectively), glued and then polished with AlO_2 polishing films of decreasing grit sizes. After this process the exposed Ag surface was cleaned with isopropyl alcohol and electroplated following the procedure in Ref. [18]. Experiments were performed with and without screens (membrane active area of 71 and 220 mm^2 respectively) resulting in a difference in the ion conductivity of approximately 6% (2.53 and 2.68 S m^{-1} with and without screen respectively at 25 °C). The active area for the experiments with the screen was analyzed from microscope pictures with Matlab. The membrane holders and screens were 3D-printed in PLA (Makertbot Replicator 2), however, with this material the electrodes holders could not be used at temperature above 45 °C. Alignment and distance between electrodes was checked by measuring the resistance between the electrodes in two different solutions (0.03 and 0.12 M LiCl solutions) mounted in the measurement cell without a membrane. From the measured resistances we estimated the misalignment/distance between the electrodes to be approximately 2–3 μm.

The in-plane ion conductivity measurements were carried out by a four-point method by placing the electrodes in the same plane of the membrane and clamping them between two glass plates. The

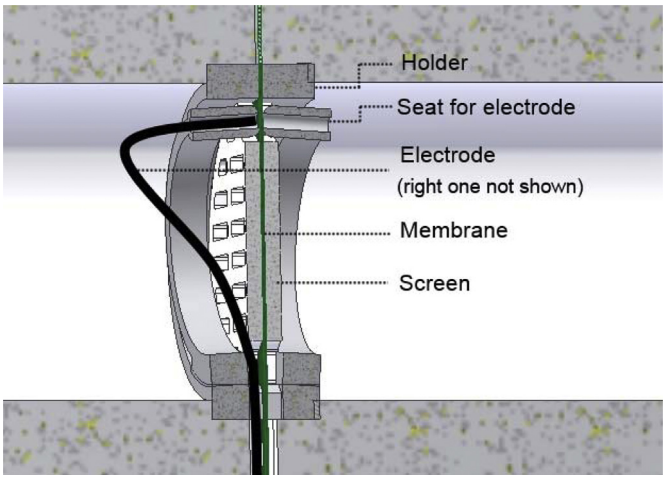

Fig. 2. Spring-loaded holders for electrodes used in-through-plane ion conductivity measurements.

Table 1
Nafion 117 properties measured in the present work: membrane thickness (δ), hydraulic permeability (κ_H), streaming potential coefficient (ν), through-plane ($\sigma_\perp$) and in-plane ($\sigma_\parallel$) ion conductivity, and the calculated *figure-of-merit* (β_{EK}), electrokinetic efficiency (η_{EK}), hydraulic permeability without electroviscous effects (κ_H^*) and power density (P/A) in the temperature range 25–70 °C and in 0.03 M LiCl solutions. β_{EK}, η_{EK}, κ_H^* and P/A were calculated by using the through-plane ion conductivity values. Power densities have been calculated considering a trans-membrane pressure difference of 10 bar. Notes: (a) interpolated and (b) extrapolated values calculated from the activation energy of the process.

T °C	δ 10^{-6} m	κ_H 10^{-17} m^2 s^{-1} Pa^{-1}	ν 10^{-9} V Pa^{-1}	$\sigma_\perp$ S m^{-1}	$\sigma_\parallel$ S m^{-1}	β_{EK}	η_{EK} %	κ_H^* 10^{-17} m^2 s^{-1} Pa^{-1}	P/A W m^{-2}
25	201	4.43	4.1	2.56	4.3[a]	1.04	17.68	8.86	0.33
30	201	5.28[a]	4.4	3.00[a]	4.9[a]	1.13	18.70	11.25	0.41
35	202	6.06	4.7[a]	3.48[a]	5.4	1.22	19.71	14.18	0.51
40	202	7.66[a]	5.0[a]	4.02	6.2	1.32	20.73	17.77	0.63
50	202	11.08	5.9	5.27[b]	7.5	1.52	22.75	27.44	0.95
60	204	15.87[a]	6.2[a]	6.81[b]	8.2	1.75	24.73	41.48	1.39
70	206	20.40	6.7	8.67[b]	9.5	1.98	26.68	61.44	1.99

distance between the reference electrodes was 12 mm, and the sample width 10 mm. The sample holder was then immersed in 0.03 M LiCl solution in a jacked borosilicate reactor and heated at the test temperature by using a water bath (Eco Gold Lauda DE).

In both cases the ion current (±1 μA to ±2 mA) was generated with an Agilent U2722A source measure unit and the potential was acquired with a NI-9219 card and recorded with Labview SignalExpress at 1.95 Hz.

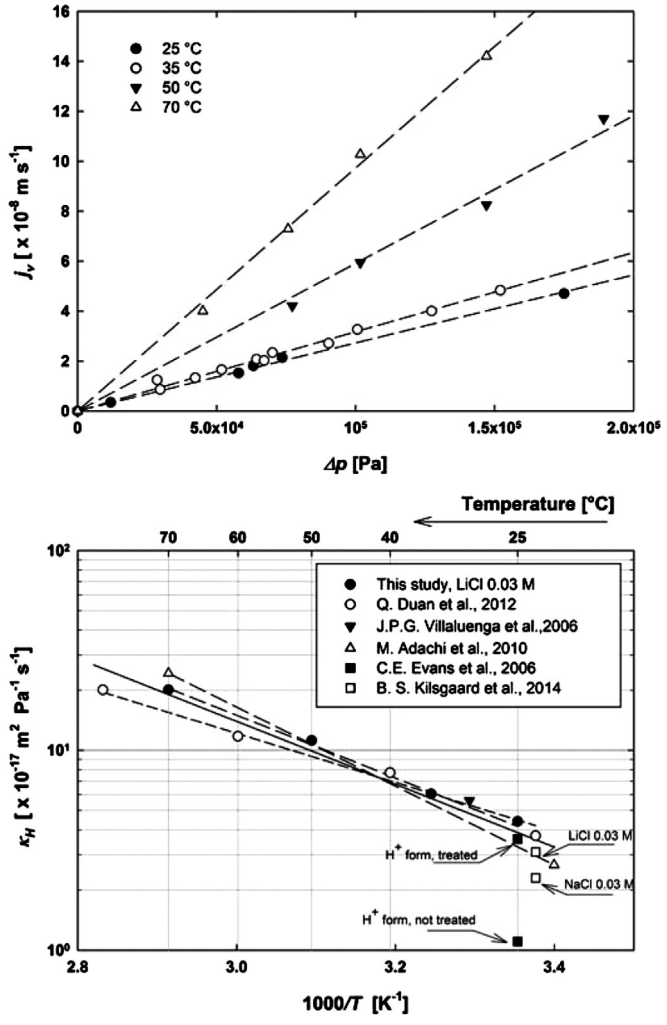

Fig. 3. Upper panel: volume fluxes as a function of the trans-membrane pressure difference in the temperature range 25–70 °C in 0.03 M LiCl solution. Lower panel: Arrhenius plot of the hydraulic permeability and comparison with literature data [18,36–39] for Nafion membranes in Li^+, Na^+ and H^+ form.

3. Results

3.1. Hydraulic permeability

The upper panel of Fig. 3 shows the volume flux, j_v, as a function of the applied pressure difference in the temperature range 25–70 °C. Pressure was applied after the temperature of the system was stabilized and the temperature difference between the high and low pressure chambers was within 0.2 °C. In both half cells the stirring rate was set to the maximum value of 900 rpm which at the same time gave better temperature stability as well as diminishing the effect of the concentration polarization. As reported in a previous work [18], the presence of a larger concentration polarization boundary layer resulted in a lower κ_H, hence the values reported in this study represent an upper limit, and should be considered as a good assessment of κ_H in the real operating conditions in a power generation device. It should also be noted that the use of these values represents a conservative way to calculate the efficiency of the system. The experiments were performed in pressure range 1 bar to approximately 3 bar and j_v was recorded after the steady state flux was reached (approximately half hour). The κ_H were calculated from the slope of the linear regressions reported in Fig. 3, constrained to pass through the origin, and the membrane thickness in the swollen state. Membrane thickness and κ_H at several temperatures are reported along with the other measured properties in Table 1. To check the consistency of the measured membrane thicknesses an additional measurement, not reported in Table 1, was carried out above the temperature range used in the present work (100 °C) finding $\delta = 211$ μm (swelling ratio of 15.2%) in rather good agreement with the measurement of Sakai et al. [32] $\delta = 220$ (swelling ratio of 18.9%) found at 100 °C in Nafion in H^+ form. Nafion in H^+ and Li^+ forms have similar water uptake [38] and consequently should have similar dimensional swelling. The value for κ_H found at 25 °C of 4.41 10^{-17} m^2 s^{-1} Pa^{-1} is somewhat larger with respect to the one found at 22 °C in the previous work 3.1 10^{-17} m^2 s^{-1} Pa^{-1} [18]. However, the slightly higher temperature in the present study can explain about half the difference. We believe that the rest, which is of the same order as the resolution of the experiment, could be explained by a better stirring in the present experimental setup and, as a consequence, a thinner boundary layer.

In the lower panel of Fig. 3, κ_H is reported as a function of temperature in an Arrhenius plot and compared with literature data for Nafion (Nafion 117 and Nafion 115) in Li^+ [18], Na^+ [18] and H^+ [36–39] form. Data at 25 °C collected by Evans et al. [38] in H^+ form are reported to highlight the difference, almost four-fold, between κ_H for the treated and untreated Nafion samples. Hence the difference in the hydraulic permeability found between our previous and current study can be also partially attributed to the slight difference in the pretreatment protocol followed.

The apparent activation energy for the hydraulic permeability of Nafion in 0.03 M LiCl solutions, E_{κ_H}, was 29.4 kJ mol^{-1}, and to the best of our knowledge it has not been reported by any other groups in the literature. However, the value found in the present study is within the one calculated by Duan et al. [37], 24.9 kJ mol^{-1} ($T = 23$–80 °C), and the one of Adachi et al. [36] of 37.8 kJ mol^{-1} ($T = 21$–70 °C) for Nafion in H^+ using pure water.

3.2. Streaming potential

As reported in one of our previous studies [18] measurements of the streaming potential coefficient with and without stirring gave the same values within 5%. In the present study we use the method without stirring only: the advantage of using this method is a more stable signal of the electrodes, and, since the experiments were conducted for a maximum of 200 s, no significant change in the temperature of the system was observed. With this method a concentration polarization layer is built up and contributes to the streaming potential. However, the intrinsic membrane contribution is time independent, whereas the contribution from concentration polarization has $\sqrt{t}$ behavior being the diffusion of ions in the solution a diffusion-limited process. Hence, the streaming potential coefficient can be found from fitting $\Delta\phi(t) = \nu\Delta p + A\sqrt{t}$ to the data [40].

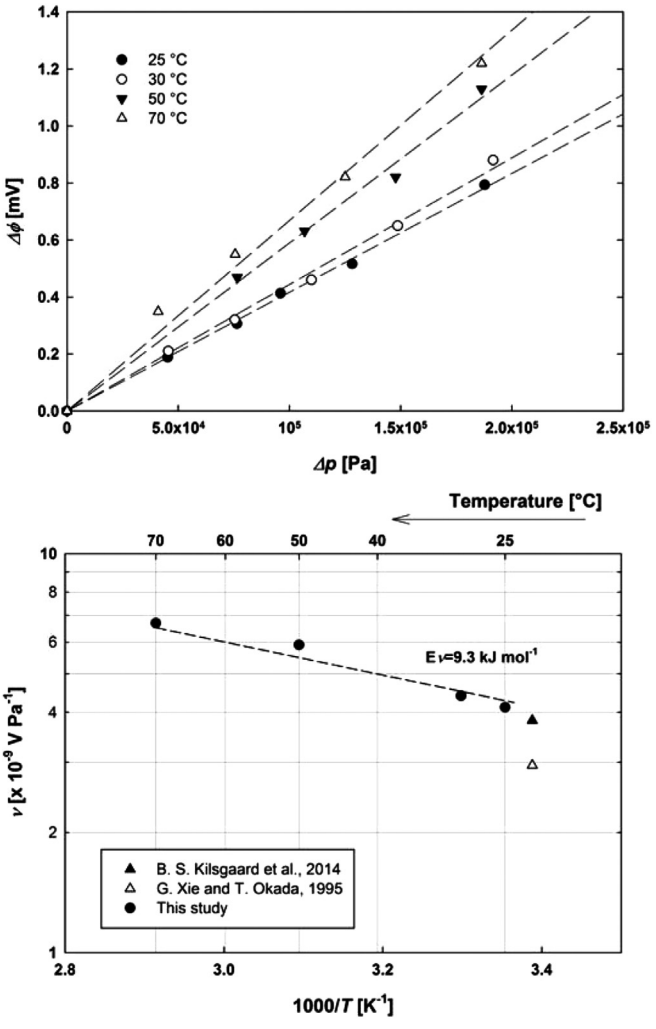

Fig. 4. Upper panel: potential difference as a function of the trans-membrane pressure difference in the temperature range 25–70 °C in 0.03 M LiCl solution. Lower panel: Arrhenius plot of the streaming potential coefficient and comparison with literature data for Nafion in 0.03 M LiCl solution at ambient temperature [18, 41].

The upper panel of Fig. 4 shows the measured streaming potential in the temperature range 25–70 °C as a function of the applied trans-membrane pressure difference. Stirring is applied until the measurement temperature is reached, but ceased before the measurement is started. From the linear regression, constrained to pass through the origin, of the streaming potential coefficients, ν are found at four different temperatures and they are shown in an Arrhenius plot in the lower panel of Fig. 4. ν varied from 4.12 10^{-9} V Pa^{-1} to 6.7 10^{-9} V Pa^{-1} at 25 °C and 70 °C, respectively. The apparent activation energy for ν (E_ν) was approximately 9.3 kJ mol^{-1}. By considering this value for the activation energy it was possible to extrapolate ν to lower temperatures. Specifically at 22 °C the extrapolated value of 4.04 10^{-9} V Pa^{-1} was fully consistent with our previous work [18] (6% higher). Compared to the value of 2.95 10^{-9} V Pa^{-1} found by Xie and Okada [41] the difference is larger and might be due to a membrane-batch dependence and/or differences in the pretreatment of the membrane as already discussed in Ref. [18].

A direct comparison of E_ν with literature data is not possible because of lack of experimental data. Nonetheless, streaming potential experiments were performed by Okada et al. [42] in Nafion 117 by using 0.03 M NaCl and 0.03 M HCl in the temperature range 25–60 °C and 25–80 °C for the two solutions, respectively. The calculated E_ν for Nafion in Na^+ and H^+ form were 3.2 and 7.3 kJ mol^{-1} respectively in the temperature range 25–60 °C. As could have been anticipated the latter value is comparable with the one retrieved in the present study, since Nafion in H^+ and Li^+ forms have similar water uptake. However, the streaming potential coefficient measured by Okada et al. [42] in Nafion in H^+ form at 80 °C was lower than the one at 60 °C. If also this data point is included in the regression for the activation energy calculation $E_\nu \approx 3.6$ kJ mol^{-1}, a value 2 ½ times lower than the one found in the present work. No explanation for the anomalous behavior of ν at 80 °C was reported by Okada et al. [42]. As mentioned previously the difference with respect to the data in Ref. [42] might be attributed to a membrane-batch dependence or a different membrane pretreatment. This interpretation is supported by the low value of the activation energy for the water permeability, 11.6 kJ mol^{-1}, in Nafion H^+ found by Okada et al. [42].

3.3. Ion conductivity

Results for ion conductivity measurements are reported in Fig. 5. The upper panel shows the ion conductivity ($\sigma_\perp$) measured through-plane with a four-electrode experimental setup in the temperature range 22–40 °C. The applied current was between −1 mA and 1 mA. Measurements at 22 °C were carried out to have a comparison with data reported by Kilsgaard et al. [18] in the same membrane and solution. In this case the agreement is excellent (2.32 S m^{-1} in the present study and 2.36 S m^{-1} in Ref. [18]). As reported in a previous study [18] literature values of σ measured in LiCl solutions ranged between 0.6 S m^{-1} and approximately 3 S m^{-1} [43–47] and the rather marked differences can be explained by the method used, the different water uptakes of the membrane and/or membrane pretreatments.

As stated earlier, measurements of $\sigma_\perp$ are limited to temperatures below 45 °C in which we calculate an activation energy ($E_{\sigma_\perp}$) of 22.9 kJ mol^{-1}. This value is close to 23.5 kJ mol^{-1} measured by Okada et al. [42] in Nafion Na^+ form with AC impedance method.

Measurements of the in-plane conductivity ($\sigma_\parallel$) were done in order to reach higher measurement temperatures. Data are shown in the lower panel of Fig. 5. Due to the different membrane sample geometry used in the in-plane experiments, the applied current

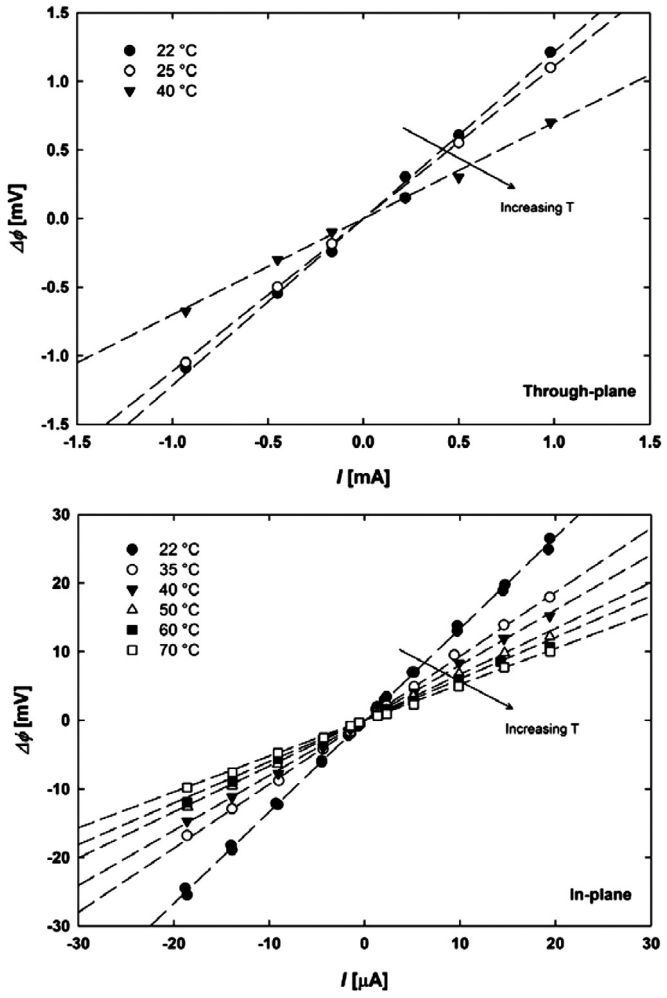

Fig. 5. Ion conductivity measurements in 0.03 M LiCl solutions. Upper panel: 4-electrode through-plane tests (22–40 °C). Lower panel: 4-electrode in-plane tests (22–70 °C).

range was greatly reduced and it was in the range −20 μA–20 μA. For $\sigma_{\parallel}$ we calculate an activation energy $E_{\sigma_{\parallel}} = 15.4$ kJ mol^{-1} as seen in Fig. 6 that is somewhat lower than $E_{\sigma_{\perp}}$. In addition it is seen that $\sigma_{\parallel}$ is systematically higher with respect to $\sigma_{\perp}$ (e.g. at 22 °C $\sigma_{\parallel} = 3.8$ S m^{-1} while $\sigma_{\perp} = 2.32$ S m^{-1}) hence $\sigma_{\parallel}$ represents an upper limit of the cation conductivity of the membrane. Proton conductivity experiments performed along and perpendicularly to the membrane extrusion axis reported by several authors [48–51] showed an anisotropic proton conductivity of Nafion which has been ascribed either to the preferential orientation at the membrane interface or to the orientation of Nafion chains along the extrusion axis. It could be suspected that the lower value of $\sigma_{\perp}$ could be a systematic error from the experimental setup where resistive contributions from the electrolyte solution would decrease the apparent$\sigma_{\perp}$. Nonetheless, we have confidence that the difference between $\sigma_{\parallel}$ and $\sigma_{\perp}$ is intrinsic. Measurements of $\sigma_{\perp}$ are reproducible (not shown) and as mentioned earlier, measurements in the cell without membrane show that misalignment of the electrodes is approximately 2–3 μm, whereby electrolyte contribution to the total cell resistance becomes negligible.

Experiments made in Nafion membrane without any preferential orientation [52] (casted Nafion NR-212) reporting isotropic conductivity substantiate the idea of the anisotropy due to the extrusion process. Also the ratio between $\sigma_{\parallel}/\sigma_{\perp}$ was proposed as an index of the degree of anisotropy of the membrane: in the present case $\sigma_{\parallel}/\sigma_{\perp}\big|_{22^{\circ}C} = 1.7$ while values of 3.6, 2.5 and 1.2 were found by Gardner and Anantaraman [49,50], Eldab et al. [48] and Soboleva et al. [51], respectively. As seen in Fig. 6 the degree of anisotropy decreases as the temperature of the system is increased. This effect can be explained because by increasing the temperature the water fraction inside the polymer increases reducing the influences of a preferential orientation. It should also be noted that isotropic conductivity (e.g. Ref. [53]) and reverse anisotropy [54] (in Nafion 112) were also found in extruded Nafion membranes.

The difference in $E_{\sigma_{\parallel}}$ and$E_{\sigma_{\perp}}$ might be a consequence of the anisotropy of the membrane considered, hence $\sigma_{\perp}$ (as well as its activation energy) should be used in the calculation of the efficiency for the electrokinetic power generation since it was measured in the same direction of the ion-transport. Therefore the extrapolated values of $\sigma_{\perp}$ in the temperature range 50–70 °C will be used for the *figure-of-merit* calculations. It should also be noted that the use of $\sigma_{\perp}$ in the calculation of the *figure-of-merit* represents a conservative way for evaluating the efficiency of the system.

4. Discussion

In Table 1 all the properties measured in the present work are reported, namely δ, κ_H, ν, $\sigma_{\perp}$ and $\sigma_{\parallel}$ and the calculated *figure-of-merit*, electrokinetic energy conversion efficiency, non-electroviscous hydraulic permeability (κ_H^*) [16] and power density (P/A) in the temperature range 25–70 °C. When the property was not measured at the specific temperature, the property has been calculated by interpolation of measured data. As reported previously, the only exception is the through-plane ion conductivity, for which at temperature equal or above 50 °C the value has been calculated by extrapolation. The calculated efficiency and power density are also reported as a function of the temperature in Fig. 7. It is worth to note, that the efficiency at room temperature, 17.7%, is close to the one found in one of our previous work (20 ± 2%) [18] at 22 °C. At 70 °C, the calculated efficiency reaches the rather high value of 26.7%, approximately 50% higher than that at 25 °C with a power density of ca. 2 W m^{-2}. By using the calculated activation

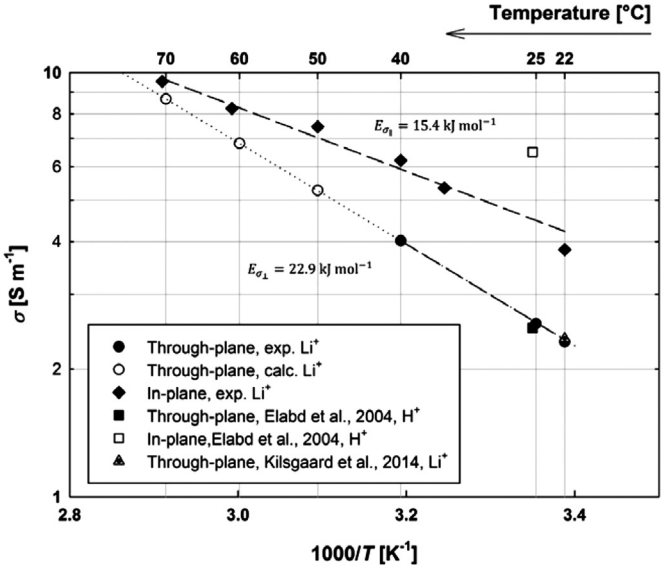

Fig. 6. Arrhenius plot of the ion conductivity measurements performed in both configurations (through-plane and in-plane) in 0.03 M LiCl solutions. For comparison data from Kilsgaard et al. [18] retrieved in Nafion 117 and same solutions have been reported (through-plane). Data from Elabd et al. [48] for proton conductivity in Nafion 117 measured with through-plane and in-plane configurations are also shown.

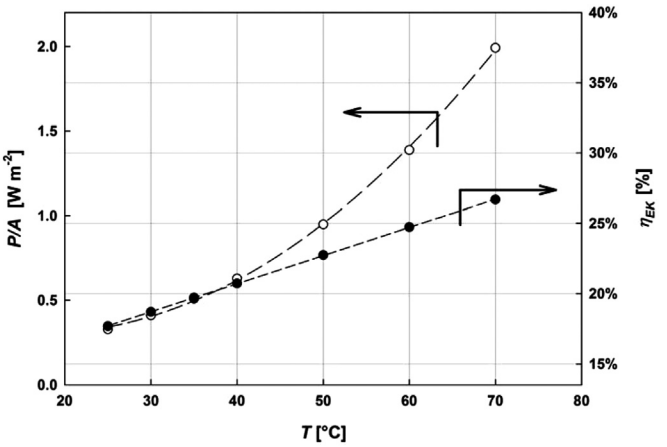

Fig. 7. Calculated electrokinetic efficiency and power density of Nafion 117 membrane in 0.03 M LiCl solution as a function of the temperature. Power densities have been calculated considering a trans-membrane pressure difference of 10 bar. Lines are a guide for the eyes.

energies, reported in Table 2 along with the pre-exponential factors, for the processes involved one can write:

$$\beta_{EK}(T) = \frac{\nu_0^2 \cdot \sigma_0}{\kappa_{H,0}} \exp\left(-\frac{2E_\nu + E_{\sigma_\perp} - E_{\kappa_H}}{RT} \right) = \frac{\nu_0^2 \cdot \sigma_0}{\kappa_{H,0}} \exp\left(-\frac{E_{\beta_{EK}}}{RT} \right) \quad (1)$$

In which $E_{\beta_{EK}}$ represents the apparent activation energy of the electrokinetic process and in the case of Nafion is approximately 12.2 kJ mol^{-1}.

The power density P/A was calculated as the work produced per unit time and area by the liquid in the membrane assuming a transmembrane pressure difference of 10 bar using the formula $P/A = \kappa_H \cdot \Delta p^2 / \delta(1 + \frac{1}{2}\beta_{EK})$; the latter expression is straightforward derived from the phenomenological equations and does also include electro-viscous effects ($\frac{1}{2}\beta_{EK}$) which increase the apparent hydraulic permeability and thereby power density, during operation. Still the calculated power density of electrokinetic power generation is low compared to fuel cells [55]. However, it can most likely be increased up to more than 100 W m^{-2} by using higher pressure difference, thinner or supported composite membranes with a very thin selective ion conductive layer. Finally Table 1 also report the non-electroviscous hydraulic permeability [16], $\kappa_H^* = \kappa_H(1 + \beta_{EK})$, which physically represents the hydraulic permeability when a current density is allowed to circulate through the membrane. The electroviscous effect arises because of the presence of charges imbedded in the membrane which influence the permeation of the liquid in the water channels; if the charges are free to move the electroviscous effect would not be present and consequently the membrane permeability would increase.

Table 2
Pre-exponential factors and activation energies for the transport properties measured in this work between ambient temperature and 70 °C. Notes: (a) measured between 22 and 40 °C.

	Pre-exponent		Activation energy kJ mol^{-1}
κ_H	6.22 10^{-12}	m^2 s^{-1} Pa^{-1}	29.4
ν	1.80 10^{-7}	V Pa^{-1}	9.3
$\sigma_\perp$ [a]	2.70 10^4	S m^{-1}	22.9
$\sigma_\parallel$	2.10 10^3	S m^{-1}	15.4
β_{EK}	1.40 10^2		12.2

The electrokinetic transport properties can be described, in a simplified way, in terms of a parallel array of straight channels, see e.g. Refs. [28,29] for a detailed derivation of the equations:

$$\kappa_H = \frac{\varphi_w r^2 \vartheta}{8\eta} \quad (2)$$

$$\nu = \frac{1}{F}\frac{f r^2}{8\eta} \quad (3)$$

$$\sigma = \frac{F^2 X \vartheta}{f} \quad (4)$$

where φ_w,r, ϑ, η, f, F and X are the volumetric fraction of water in the polymer, average radius of the pore, the tortuosity of the matrix, the viscosity of the aqueous solution, the frictional coefficient, the Faraday constant and the charge density per unit volume of the membrane, respectively.

The κ_H is estimated by the average radius dimension in which the volume flux takes place, not considering the friction between the water passing through the membrane and the counter-ion that are considered fixed. It also worth to note that in general the ion conductivity can be expressed as the sum of the terms related with the bulk concentration of ions in the solution and the counterions shielding the surface charge. However in the presence of very dilute solutions the contribution of the former term to the total ion conductivity can be considered negligible [56].

Eqs. (2) and (3) can be separately used to have two independent estimations of the pore size of a charged membrane even if some additional information on the membrane characteristics are needed: i.e. volumetric fraction of water and the tortuosity of the water channels in the polymeric matrix. However, in first approximation, ϑ can be set equal to one as in Ref. [57] and the volumetric fraction of water can be derived by the knowledge of the linear swelling under the hypothesis of isotropic volume dilation. By considering the equation for the frictional coefficient, $f = RT/D_{Li}$ in which $D_{Li} = D_{Li,0}\exp(-E_{diff\ Li}/RT)$ represents the diffusion coefficient of Li^+, it is thus possible to estimate the average pore size of the parallel array using, as further simplification, for η the value in pure water and for $D_{Li,0}$ and $E_{diff\ Li}$ the one in dilute aqueous solutions 2.76 10^{-6} m^2 s^{-1} and 19.5 kJ mol^{-1}, respectively [58–60].

These calculations have been reported in terms of average pore size of the water channel in Fig. 8 as a function of the temperature. The pore size diameter increases from roughly 2.0 to 2.8 nm in the temperature range 25–70 °C assuming similar values for the two independent measurements. This latter evidence substantiates the internal consistency of the hydraulic permeability and streaming potential coefficient values found in the present work. Indeed by combining Eqs. (2) and (3):

$$\frac{\kappa_H}{\nu} \equiv \frac{\kappa_{H,0}}{\nu_0} exp\left(-\frac{E_{\kappa_H} - E_\nu}{RT} \right) = \frac{\varphi_w F}{RT} D_{Li,0} \exp\left(-\frac{E_{diff\,Li}}{RT} \right) \quad (5)$$

it is apparent that the temperature dependence of the ratio between the hydraulic permeability and streaming potential coefficient should be similar to the activation energy of the diffusion coefficient of lithium ion (neglecting the slight temperature dependence of φ_w). From the experiments reported in the present work $E_{\kappa_H} - E_\nu$ = 20.1 kJ mol^{-1} and resulted similar to $E_{diff\ Li}$ = 19.5 kJ mol^{-1}.

It should be pointed out that the calculated pore dimensions are not representative of the real structure of Nafion membranes but can be used to compare the performances of different charged membranes. The same figure also reports results from Schmidt-

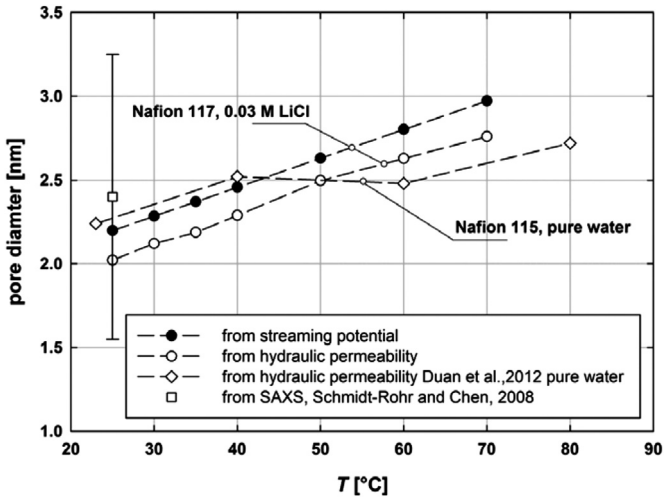

Fig. 8. Esteemed average pore diameters from the analysis of the streaming potential and hydraulic permeability measurements assuming a parallel array of straight channels. For comparison sake are also reported the calculated size from analysis of SAXS experiments in Nafion H^+ form at 20% vol of water by Schmidt-Rohr and Chen [27] and from hydraulic permeability in pure water by Duan et al. [37] in Nafion 115.

Rohr and Chen [27] retrieved from SAXS data on Nafion membrane by using parallel water-channel model simulations. In Ref. [27] the authors used long straight parallel channels in cylindrical inverted micelles model, able to reproduce the characteristic SAXS features at different hydration levels. In that study channels diameters from 1.8 to 3.5 nm, with an average of 2.4 nm, were found at 20% vol. ($\lambda = 6.7 \mathrm{mol_{H_2O}/mol_{SO_3H^-}}$) so at a hydration level well below the one used in this work. However the pore diameters calculated in the present work are of the same order of magnitude, compatible with the believed structure of Nafion [22–24] and with the calculated average dimensions from hydraulic permeability measurements by Duan et al. [37].

In addition Eq. (4) can be used to critically discuss the ion conductivity values used in the electrokinetic efficiency calculations since it only requires the knowledge of the diffusion coefficient of Li^+ and the charge density per unit volume of the swollen membrane. This latter quantity can be expressed as a function of the volume dilation, the ion exchange capacity, *IEC*, and the dry polymer density ρ_{pol}: $X = IEC \times \rho_{pol}/(1 + \Delta V/V)$. The calculated values of σ are higher than the one extrapolated from the experimental results (48.3% and 17.3% higher at 50 and 70 °C respectively) hence the latter represent a conservative way for evaluating the efficiency of the system.

Finally the set of equations can be substituted in Eq. (1) obtaining:

$$\beta_{EK} = \frac{fr^2}{8\eta}\frac{X}{\varphi_w} \tag{6}$$

This equation can be used as a first approximation of the electrokinetic efficiency of an ionomeric membrane by the knowledge of its pore size, dry density, volume dilation and ion exchange capacity. Also it substantiates the idea that charged membranes with larger pore size, such as collodion cation exchange membranes or modified Nafion, would have higher efficiency as well as power density.

5. Conclusions

The main goal of the present study was to measure the electrokinetic power generation efficiency of Nafion membranes at different temperatures. In the temperature range 25 °C–70 °C, the activation energies, of three electrokinetic transport properties, namely hydraulic permeability, streaming potential coefficient and ion conductivity in 0.03 M LiCl solutions were measured (29.4 kJ mol^{-1}, 9.3 kJ mol^{-1} and 22.9 kJ mol^{-1} respectively). The efficiency was evaluated from the electrokinetic *figure-of-merit* and showed a monotonous increase between about 17.7 and 26.6% by increasing the temperature of the system from 25 °C to 70 °C. From a simple model, that considers the Nafion membrane as an array of cylindrical parallel channels in which the transport takes place, it was possible to calculate the average channel diameters. This latter property was shown to vary between approximately 2.0–2.8 nm (at 25 °C and 70 °C respectively) in rather good agreement with the believed microstructure of Nafion membrane in swollen state. These calculations additionally showed that using membranes with larger pore size could eventually result in higher power generation efficiency.

Acknowledgment

The authors gratefully acknowledge the financial support of the Villum Foundation (grant number: VKR022356) through the Young Investigator Programme and Aarhus University Research Foundation through AU Ideas Programme. The authors would also like to thank Erik Ejler Pedersen of the Department of Chemistry, Aarhus University for the constant technical support.

Nomenclature

D_{Li}	diffusion coefficient of Li^+, $m^2\ s^{-1}$
$D_{Li,0}$	pre-exponential factor for the diffusion coefficient of Li^+, $m^2\ s^{-1}$
E	activation energy, J mol^{-1}
F	Faraday constant, 96,485 C mol^{-1}
f	frictional coefficient, J s mol^{-1} m^{-2}
I	ion current, A
IEC	ion exchange capacity, mol kg^{-1}
j_v	volume flux, m s^{-1}
Δp	trans-membrane differential pressure, Pa
P/A	power density, W m^{-2}
R	ideal gas constant, J mol^{-1} K^{-1}
r	pore radius, m
T	temperature, K
X	charge density per unit volume, mol m^{-3}
$\Delta V/V$	volume dilation

Greek symbol

β_{EK}	electrokinetic *figure-of-merit*
δ	membrane thickness, m
η	viscosity, Pa s
η_{EK}	electrokinetic efficiency
ϑ	tortuosity of the matrix
κ_H	hydraulic permeability, $m^2\ s^{-1}\ Pa^{-1}$
$\kappa_{H,0}$	pre-exponential factor hydraulic permeability, $m^2\ s^{-1}\ Pa^{-1}$
λ	solution uptake, $\mathrm{mol_{H_2O}(mol_{SO_3H^-})^{-1}}$
ν	streaming potential coefficient, V Pa^{-1}
ν_0	pre-exponential factor streaming potential coefficient, V Pa^{-1}
ρ	density, kg m^{-3}
σ	ion conductivity, S m^{-1}
σ_0	pre-exponential factor ion conductivity, S m^{-1}
σ_q	charge density, C m^{-2}
φ	volumetric fraction
ϕ	streaming potential, V

Superscripts

*	referred to intrinsic

Subscripts

diff Li	referred to diffusion coefficient of Li^+
pol	referred to polymer in dry condition
w	referred to water
β_{EK}	referred to electrokinetic *figure-of-merit*
κ_H	referred to hydraulic permeability
ν	referred to streaming potential coefficient
σ	referred to ion conductivity
$\perp$	referred to through-plane experiments
$\parallel$	referred to in-plane experiments

References

[1] J. Li, M. Pan, H. Tang, RSC Adv. 4 (2014) 3944–3965.
[2] O. Savadogo, J. Power Sources 127 (2004) 135–161.
[3] P. Costamagna, S. Srinivasan, J. Power Sources 102 (2001) 242–252.
[4] P. Costamagna, S. Srinivasan, J. Power Sources 102 (2001) 253–269.
[5] K.D. Kreuer, J. Membr. Sci. 185 (2001) 29–39.
[6] S.J. Hamrock, M.A. Yandrasits, J. Macromol. Sci. Polym. Rev. 46 (2006) 219–244.
[7] F.A. Morrison, J.F. Osterle, J. Chem. Phys. 43 (1965) 2111–2115.
[8] R.J. Gross, J.F. Osterle, J. Chem. Phys. 49 (1968) 228–234.
[9] D. Burgreen, F.R. Nakache, J. Phys. Chem. 68 (1964) 1084–1091.
[10] D. Burgreen, F.R. Nakache, J. Appl. Mech. 32 (1965) 675–679.
[11] J. Yang, F.Z. Lu, L.W. Kostiuk, D.Y. Kwok, J. Micromech. Microeng. 13 (2003) 963–970.
[12] F.H.J. van der Heyden, D.J. Bonthuis, D. Stein, C. Meyer, C. Dekker, Nano Lett. 7 (2007) 1022–1025.
[13] A.M. Duffin, R.J. Saykally, J. Phys. Chem. C 111 (2007) 12031–12037.
[14] A.M. Duffin, R.J. Saykally, J. Phys. Chem. C 112 (2008) 17018–17022.
[15] Y. Xie, X. Wang, J. Xue, K. Jin, L. Chen, Y. Wang, Appl. Phys. Lett. 93 (2008) 163116.
[16] A. Bentien, T. Okada, S. Kjelstrup, J. Phys. Chem. C 117 (2013) 1582–1588.
[17] C.E. Evans, R.D. Noble, C.A. Koval, Ind. Eng. Chem. Res. 45 (2005) 472–475.
[18] B.S. Kilsgaard, S. Haldrup, J. Catalano, A. Bentien, J. Power Sources 247 (2014) 235–242.
[19] D.M. Rowe, Thermoelectrics Handbook: Macro to Nano, CRC, Boca Raton, FL, 2006.
[20] W.H. Koh, H.P. Silverman, J. Membr. Sci. 13 (1983) 279–290.
[21] P.N. Pintauro, R. Tandon, L. Chao, W. Xu, R. Evilia, J. Phys. Chem. 99 (1995) 12915–12924.
[22] T.D. Gierke, G.E. Munn, F.C. Wilson, J. Polym. Sci. Part B Polym. Phys. 19 (1981) 1687–1704.
[23] G. Gebel, J. Lambard, Macromolecules 30 (1997) 7914–7920.
[24] H.G. Haubold, T. Vad, H. Jungbluth, P. Hiller, Electrochim. Acta 46 (2001) 1559–1563.
[25] M.H. Litt, Ab. Pap. Am. Chem. Soc. 38 (1997) 80–81.
[26] M.H. Kim, C.J. Glinka, S.A. Grot, W.G. Grot, Macromolecules 39 (2006) 4775–4787.
[27] K. Schmidt-Rohr, Q. Chen, Nat. Mater. 7 (2008) 75–83.
[28] O. Kedem, A. Katchalsky, Trans. Faraday Soc. 59 (1963) 1918–1930.
[29] O. Kedem, A. Katchalsky, Trans. Faraday Soc. 59 (1963) 1931–1940.
[30] A.M. Herring, J. Macromol. Sci. Polym. Rev. 46 (2006) 245–296.
[31] A.D. Liyanage, J.P. Ferraris, I.H. Musselman, D.-J. Yang, T.E. Andersson, D.Y. Son, K.J. Balkus Jr., J. Membr. Sci. 392–393 (2012) 175–180.
[32] T. Sakai, H. Takenaka, N. Wakabayashi, Y. Kawami, E. Torikai, J. Electrochem. Soc. 132 (1985) 1328–1332.
[33] A. Parthasarathy, S. Srinivasan, A.J. Appleby, C.R. Martin, J. Electrochem. Soc. 139 (1992) 2856–2871.
[34] J.T. Hinatsu, M. Mizuhata, H. Takenaka, J. Electrochem. Soc. 141 (1994) 1493–1498.
[35] T.A. Zawodzinski, C. Derouin, S. Radzinski, R.J. Sherman, V.T. Smith, T.E. Springer, S. Gottesfeld, J. Electrochem. Soc. 140 (1993) 1041–1047.
[36] M. Adachi, T. Navessin, Z. Xie, F.H. Li, S. Tanaka, S. Holdcroft, J. Membr. Sci. 364 (2010) 183–193.
[37] Q. Duan, H. Wang, J. Benziger, J. Membr. Sci. 392–393 (2012) 88–94.
[38] C.E. Evans, R.D. Noble, S. Nazeri-Thompson, B. Nazeri, C.A. Koval, J. Membr. Sci. 279 (2006) 521–528.
[39] J.P.G. Villaluenga, B. Seoane, V.M. Barragan, C. Ruiz-Bauza, J. Membr. Sci. 274 (2006) 116–122.
[40] T. Okada, S.K. Ratkje, H. Hanche-Olsen, J. Membr. Sci. 66 (1992) 179–192.
[41] G. Xie, T. Okada, Electrochim. Acta 41 (1996) 1569–1571.
[42] T. Okada, G. Xie, M. Meeg, Electrochim. Acta 43 (1998) 2141–2155.
[43] K. Asaka, N. Fujiwara, K. Oguro, K. Onishi, S. Sewa, J. Electroanal. Chem. 505 (2001) 24–32.
[44] I.A. Stenina, P. Sistat, A.I. Rebrov, G. Pourcelly, A.B. Yaroslavtsev, Desalination 170 (2004) 49–57.
[45] T. Okada, G. Xie, O. Gorseth, S. Kjelstrup, N. Nakamura, T. Arimura, Electrochim. Acta 43 (1998) 3741–3747.
[46] M. Doyle, M.E. Lewittes, M.G. Roelofs, S.A. Perusich, R.E. Lowrey, J. Membr. Sci. 184 (2001) 257–273.
[47] L. Chaabane, G. Bulvestre, C. Larchet, V. Nikonenko, C. Deslouis, H. Takenouti, J. Membr. Sci. 323 (2008) 167–175.
[48] Y.A. Elabd, C.W. Walker, F.L. Beyer, J. Membr. Sci. 231 (2004) 181–188.
[49] C.L. Gardner, A.V. Anantaraman, J. Electroanal. Chem. 395 (1995) 67–73.
[50] C.L. Gardner, A.V. Anantaraman, J. Electroanal. Chem. 449 (1998) 209–214.
[51] T. Soboleva, Z. Xie, Z. Shi, E. Tsang, T. Navessin, S. Holdcroft, J. Electroanal. Chem. 622 (2008) 145–152.
[52] K.R. Cooper, ECS Trans. 41 (2011) 1371–1380.
[53] R.F. Silva, M. De Francesco, A. Pozio, J. Power Sources 134 (2004) 18–26.
[54] O. Yamada, Y. Yin, K. Tanaka, H. Kita, K.-i. Okamoto, Electrochim. Acta 50 (2005) 2655–2659.
[55] G. Hoogers, Fuel Cell Technology Handbook, CRC Press, Boca Raton, 2003.
[56] R.M.M. Smeets, U.F. Keyser, D. Krapf, M.Y. Wu, N.H. Dekker, C. Dekker, Nano Lett. 6 (2006) 89–95.
[57] Q. Zhao, P. Majsztrik, J. Benziger, J. Phys. Chem. B 115 (2011) 2717–2727.
[58] G. Xie, T. Okada, J. Electrochem. Soc. 142 (1995) 3057–3062.
[59] K. Tanaka, M. Nomura, J. Chem. Soc. Faraday Trans. 1 (83) (1987) 1779–1782.
[60] A.V. Egorov, A.V. Komolkin, V.I. Chizhik, P.V. Yushmanov, A.P. Lyubartsev, A. Laaksonen, J. Phys. Chem. B 107 (2003) 3234–3242.